Bulletin of Glaciological Research 33 (2015) 7–14
doi: 10.5331/bgr.33.7

Glaciological and meteorological observations at the SIGMA-D site, northwestern Greenland Ice Sheet

Sumito MATOBA[1], Hideaki MOTOYAMA[2,3], Koji FUJITA[4], Tetsuhide YAMASAKI[5], Masahiro MINOWA[1,6], Yukihiko ONUMA[7], Yuki KOMURO[8], Teruo AOKI[9], Satoru YAMAGUCHI[10], Shin SUGIYAMA[1] and Hiroyuki ENOMOTO[2,3]

1 Institute of Low Temperature Science, Hokkaido University, Sapporo 060–0819, Japan
* matoba@pop.lowtem.hokudai.ac.jp
2 National Institute of Polar Research, Tachikawa, Tokyo 190–8518, Japan
3 SOKENDAI (The Graduate University for Advanced Studies), Tachikawa, Tokyo 190–8518, Japan
4 Graduate School of Environmental Studies, Nagoya University, Nagoya 464–8601, Japan
5 Avangnaq, Takatsuki 596–0094, Japan
6 Graduate School of Environmental Science, Hokkaido University, Sapporo 060–0810, Japan
7 Graduate School of Science, Chiba University, Chiba 263–8522, Japan
8 Graduate School of Science and Engineering, Yamagata University, Yamagata 990–8560, Japan
9 Meteorological Research Institute, Tsukuba 305–0052, Japan
10 Snow and Ice Research Center, National Research Institute of Earth Science and Disaster Prevention, Nagaoka 940–0821, Japan

(Received August 30, 2015; Revised manuscript accepted November 10, 2015)

Abstract

During spring 2014, we drilled an ice core on the northwestern Greenland Ice Sheet, recovering a core of total length 225 m. We also conducted stratigraphic observations, measurements of the density of the ice core, near-infrared photography of the ice core, preparation of liquid samples for chemical analysis, and measurements of borehole temperature. The pore close-off depth was 60 m, and the temperature in the borehole was −25.6 ℃ at a depth of 10 m. In addition, we conducted snow-pit observations, ice-velocity and surface-elevation measurements using the global positioning system (GPS), meteorological observations, and installation of an automated weather station (AWS).

Key words: Greenland Ice Sheet, ice core, ice velocity, automated weather station, Qaanaaq

1. Introduction

The Greenland Ice Sheet (GrIS) has been losing mass at an accelerating rate since the 1990s (*e.g.*, van den Broeke *et al.*, 2009; Rignot *et al.*, 2011). Remote-sensing and numerical-modeling studies indicate that the current loss of mass of the GrIS is because of an increase in surface melt and ice discharge from marine-terminating outlet glaciers (Sasgen *et al.*, 2012; Enderlin *et al.*, 2014; Khan *et al.*, 2014). To investigate the processes of the mass loss of the northwestern GrIS, several glaciological and meteorological observations have been conducted under two scientific projects since 2011. The Snow Impurity and Glacial Microbe effects on abrupt warming in the Arctic project (SIGMA), which focuses on the surface melting of the GrIS and the snow/albedo feedback effect caused by snow grain growth and light-absorbing snow/ice impurities, has conducted meteorological and glaciological observations on the northwestern GrIS (Aoki *et al*, 2014; Yamaguchi *et al.*, 2014a). The Green Network of Excellence Arctic Climate Change Research Project (GRENE-Arctic) focuses on processes that occur near the coast, including the dynamics of tidewater glaciers and the loss of mass of ice caps (Sugiyama *et al.*, 2014; 2015).

We conducted ice-core drilling as well as glaciological and meteorological observations to investigate accumulation processes and reconstruct paleo-environmental changes in the region of the accumulation area of the northwestern part of the GrIS covered by SIGMA and GRENE-Arctic.

2. Research Area

The observation site (77.636°N, 59.120°W, 2100 m a.s.l.), called SIGMA-D, is located 250 km east of the town of Qaanaaq in northwestern Greenland, and lies in the upstream section of the Heilprin Glacier, the largest outlet glacier in the Qaanaaq area, which discharges into Inglefield Bredning (Fig. 1). The distance from the observation site to the terminus of Heilprin Glacier was approximately 170 km. The ice velocity of the Heilprin

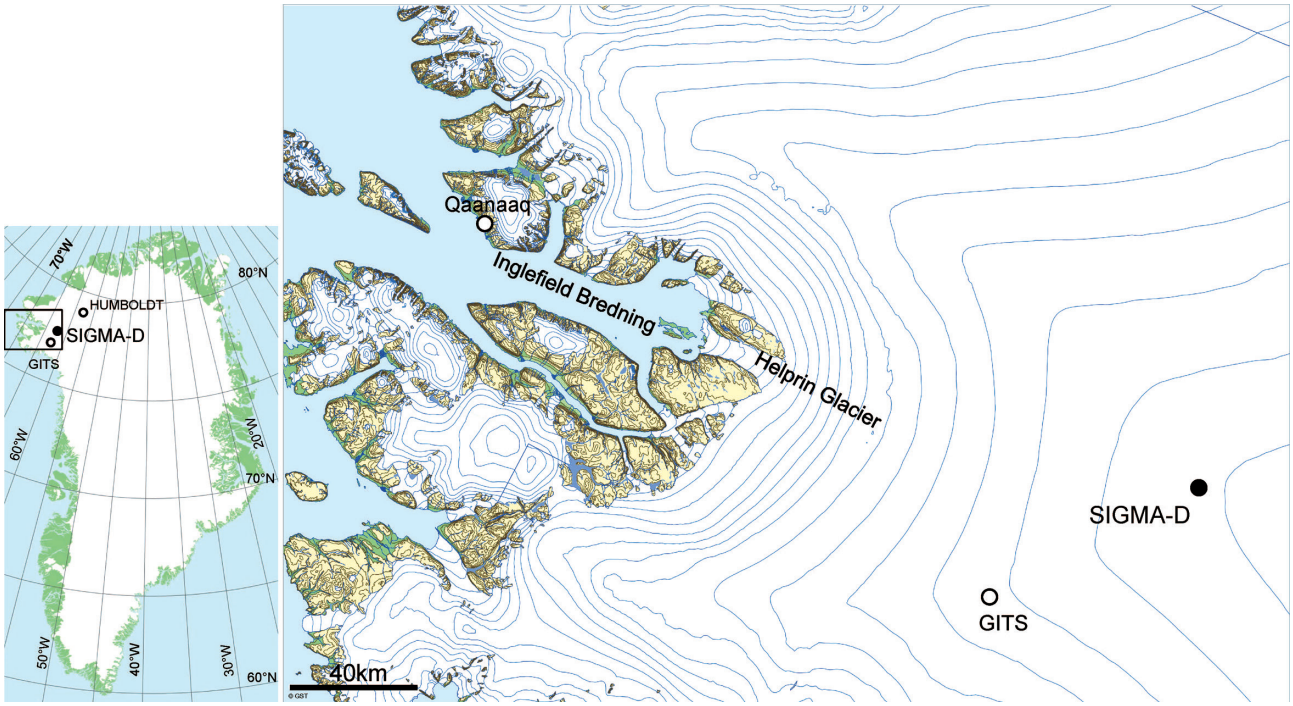

Fig. 1. Location of the SIGMA-D site (77.636°N, 59.120°W, 2100 m a.s.l.).

Glacier increased by 18 % between 2000 and 2005 (Rignot and Kanagaratnam, 2006). In the 1990s, the Program for Arctic Regional Climate Assessment (PARCA) project obtained ice cores near our observation site (Bales *et al.*, 2001). The annual accumulation at the ice-core sites (GITS; 77.1°N, 61°W, 1868 m a.s.l., HUMBOLDT; 78.5°N, 56.8°W, 1998 m a.s.l) has been estimated from ice-core analyses to be 34.4 (1957–1995) and 14.7 (1957–1994) g cm^{-2} a^{-1}, respectively.

3. Participants

This project was launched as a collaborative program between SIGMA and GRENE-Arctic. The project participants were as follows:
Dr. Hideaki Motoyama (National Institute of Polar Research), Leader and Chief Driller
Dr. Sumito Matoba (Institute of Low Temperature Science, Hokkaido Univ.), logistics and sample processing
Dr. Koji Fujita (Nagoya Univ.), ice-core processing and GPS survey
Mr. Tetsuhide Yamasaki (Avangnaq), Chief of Logistics, risk management, and driller
Mr. Masahiro Minowa (Hokkaido Univ.), GPS survey and ice-core processing
Mr. Yukihiko Onuma (Chiba Univ.), ice-core processing
Mr. Yuki Komuro (Yamagata Univ.), ice-core and sample processing
Dr. Teruo Aoki (Meteorological Research Institute), ground support in Japan and Qaanaaq
Dr. Satoru Yamaguchi (Snow and Ice Research Center, National Research Institute of Earth Science and Disaster Prevention), AWS preparation, ground support in Japan

4. Itinerary

The itinerary is summarized in Table 1. We chartered a Twin Otter (de Havilland, Canada, DHC-6) airplane from Kenn Borek Air, Ltd. in Resolute Bay, Canada, and flew personnel and equipment from Qaanaaq, Greenland, to the drilling site on 5 May 2014. Three flights were required to transport seven people and approximately 1,800 kg of equipment, including food and fuel. We set up our camp on 5 May and stayed until 3 June. All scheduled field studies were accomplished by 26 May. However, we had to wait for the pick-up flights until 3 June because of bad weather in Qaanaaq and Resolute Bay. On 3 June, we flew all personnel, equipment, and ice core sections totaling 222.72 m long from the observation site to Qaanaaq in the same Twin Otter that we had used on 5 May, which required two flights. The ice cores, accompanied by two personnel (Motoyama and Yamasaki), were transported from Qaanaaq to Resolute Bay on one flight with the Twin Otter and were temporarily stored in a freezer at the Polar Continental Shelf Program in Resolute Bay until 5 June. The frozen ice cores were transported from Resolute Bay to the National Institute of Polar Research (NIPR) in Tachikawa, Tokyo, on 16 June via Iqaluit, Ottawa, and Toronto in Canada and Narita in Japan.

5. Campsite

Our camp included a drilling tent, kitchen tent, food-storage tent, seven sleeping tents, a toilet tent, a tent for sample melting, and a snow cave trench for ice-core pro-

Table 1. Dates of field studies and logistics.

Site / Date	RES	QNQ	SIGMA-D Drilling	Processing	Observations
4-May	A Twin Otter flight				
5-May		Equipment transported by 3 Twin Otter flights	Set up camp / Set up a drill system		
6-May				Construct snowhall labo	GPS static mes. on Drill site
7-May			Drilling		
8-May				Ice core processing	
10-May					Install AWS
11-May					GPS position mes. of stakes in the flow field
12-May				Sample melting	
14-May					Snow pit
20-May					
21-May			Bore hole temp. mes.		GPS Surface topograpy mes.
22-May			Closing drill camp		
24-May					
25-May				Closing snowhall labo	GPS position mes. of stakes in the flow field
26-May					
27-May			Postponement of pick up because of bad weather in Resolute Bay		
28-May					
2-Jun	A Twin Otter flight		Closing tent for food		
3-Jun			Closing main tent and personal tents		
		Ice cores, samples personnels and equipment transported by 3 Twin Otter flights			
	Ice cores and 2 persons by 1 Twin Otter flight				
5-Jun	Ice cores were transported to Japan through Iqualit and Ottawa.				

RES: Resolute Bay
QAQ: Qaanaaq

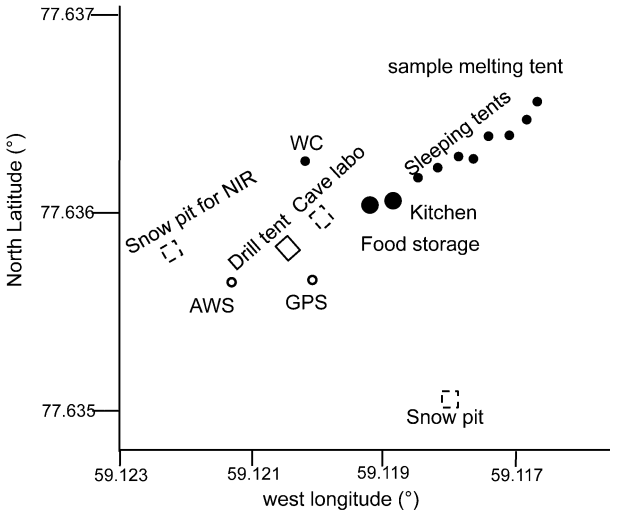

Fig. 2. Map of campsite.

cessing, as shown in Fig. 2. The GPS position of the drilling site was 77.636°N, 59.120°W. We dug a snow cave trench (2.5×5 m, 2 m deep), which was covered with plywood and vinyl sheets. In this trench, we constructed a 5-m-long worktable and installed a platform for near-infrared (NIR) photography designed by MRI and Prede Co., Ltd., and a band saw (REXON, model BS-10). Processing of the ice core was carried out in the trench.

Table 2. Specifications of ice drilling system.

Drill	
Diameter (inner/outer)	95/129 mm
Average core length	50 cm
Maximum core length	70 cm
Drill / Barrel length	2133 mm / 1340 mm
Drill motor	DC 100 V, 350 W
Type of anti-torque	Leaf spring type
Mast and Winch system	
Mast type	Aluminum tower
Mast height	2675 mm
Winch motor	DC 90 V 1.0 kW
Cable	Armored 250 m, diameter 4.72 mm

6. Field activities

6.1 Ice-core drilling

After establishing the drilling tent and drilling facilities, we began drilling the ice core on the afternoon of 7 May and completed drilling on 20 May. We used an electromechanical ice-core drilling system newly developed by Geotech Co., Ltd., Nagoya, Japan. The specifications of the drilling system are shown in Table 2. We used a generator (YAMAHA model EF2300i) with a four-cycle, single-cylinder gasoline engine for the drilling operations. For high-elevation use, we replaced the fuel spray nozzle in the carburetor with one with a smaller

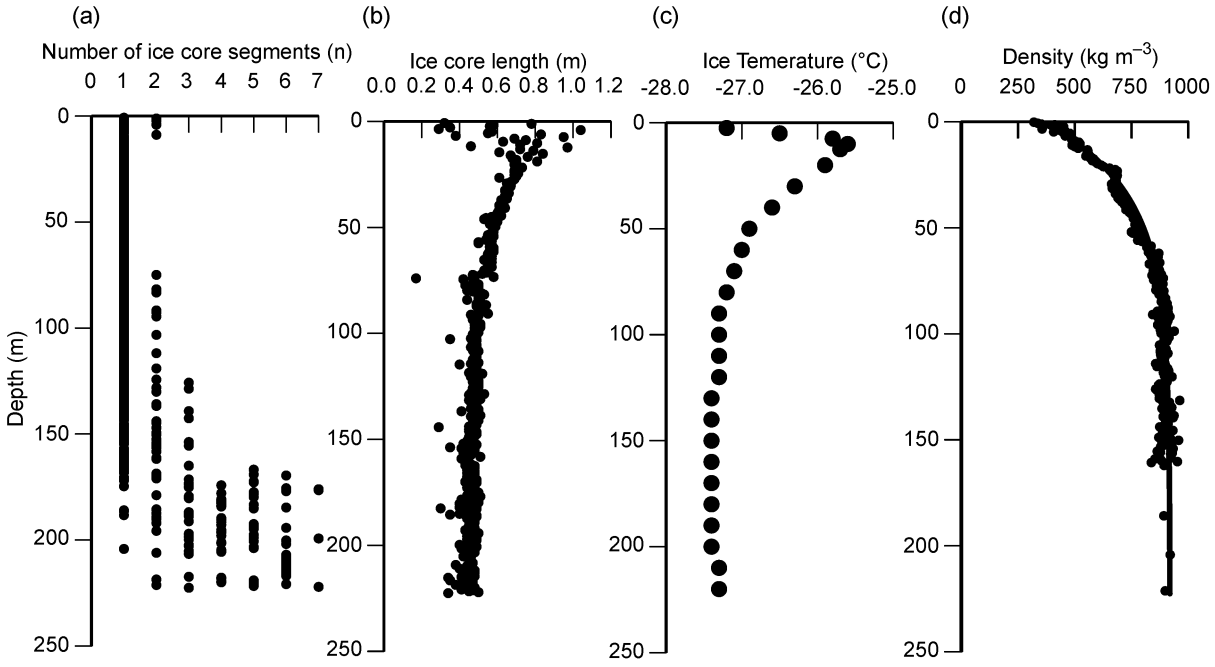

Fig. 3. Depth profile of (a) segments of ice core, (b) total ice-core length (bottom) obtained from one drill run, (c) temperature profile of the borehole wall, and (d) density profile of the ice core and approximation by dry snow densification (Schytt, 1958).

hole. To prevent the air intake from closing up due to freezing of the air filter in the low temperatures, we removed the air filter made of sponge from the air filter unit. To prevent the carburetor from freezing, we attached a metal plate from the exhaust muffler to the carburetor to conduct heat to the carburetor.

On 20 May, we finished drilling the ice core at a depth of 222.72 m, after 441 completed drilling runs. Figs. 3a and 3b show the depth profiles of a number of ice-core segments and the total length of all ice-core sections obtained by one drilling run. The number of ice-core segments increased at depths below 165 m, and their average length over the entire depth of the core was ~0.5 m. The depth range over which the number of segments increases is called brittle-ice. The air pressure of the air bubbles in ice cores increases below 100-m depth, leading to brittleness of the core. The brittle-ice problem is well known, and often appears at depths below 100–150 m in alpine glaciers, small ice caps, and ice sheets (*e.g.*, Takahashi, 1996; Motoyama *et al.*, 2001; Koci, 2002; Matoba *et al.*, 2014). To avoid this problem, we attempted the following: (1) changing the strength of the spring to prevent damage by the core catcher; (2) changing the rake angle of the cutter and height of the shoe to reduce the shock to the ice; (3) reducing the cutter load by adjusting the winch speed; (4) changing the cutter position to change the clearance between the core barrel and ice core, reducing friction between the barrel and ice core; and (5) changing separators between the chip chamber and the ice-core chamber in the barrel to avoid penetration of the ice core chip into the ice-core chamber. However, none of these modifications solved the problem.

6.2 Borehole temperature measurement

We measured the ice temperature of the borehole wall from 21 to 22 May after completion of the ice-core drilling. The ice temperature was measured with a thermistor sensor (Techno-seven model BYE-64) that was kept in direct contact with the wall of the borehole by leaf springs (Kameda *et al.*, 1993). The resistance of the sensor was measured using a digital multimeter (Fluke model 106) at a resolution of 10 ohms and an accuracy of 0.5 %. The ambient temperature was −10 to 0 ℃. The temperature of the wall of the borehole was calculated by a following equation (Shiraiwa *et al.*, 2003).

$$T = -20.878 \ln(R) + 51.75, \quad (1)$$

where T (℃) is the temperature of the wall of borehole and R (kΩ) is the resistance measured by the digital multimeter. The sensor was inserted into the borehole and left for 25 min at the setting depth. The vertical profile of the temperature is shown in Fig. 3c. The temperature at 10-m depth was −25.6 ℃.

6.3 Ice-core processing and ice-core properties

We established a snow-cave trench for ice-core processing on 8 May and conducted stratigraphic observations of the ice core, measurements of its density, NIR photography of the ice core, and preparations for chemical analysis in the trench. The schematic diagram of ice core cutting for ice core analyses is shown in Fig. 4.

We recorded the stratigraphic features of the ice core on chart sheets at real scale using a light table over the entire depth of the core, and measured the diameter, length, and weight of each ice-core segment from the surface to 161-m depth continuously and at 161.90–162.32, 185.63–186.11, 204.04–204.49, and 221.04–221.5 m, to calcu-

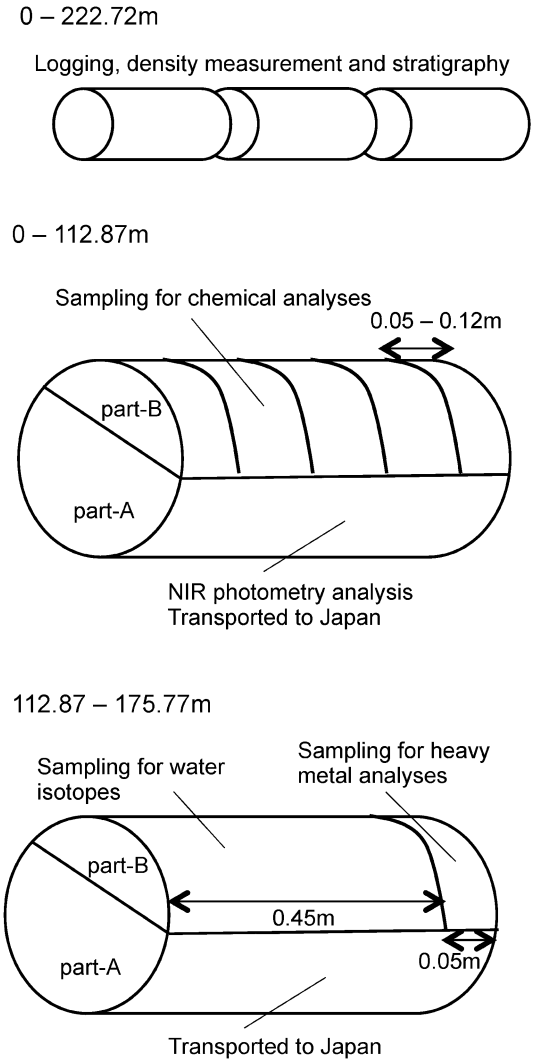

Fig. 4. Schematic diagram of ice core cutting for ice core analyses.

late its density (Fig. 3d). The density of the ice core was approximated by the experimental densification equation of dry snow (Schytt, 1958).

$$\rho(z) = \rho_i - [\rho_i - \rho_s] \exp(-z/(z_t/1.9)), \quad (2)$$

where ρ_i (kg m^{-3}) is the density of ice, ρ_s (kg m^{-3}) is the density of surface snow, and z_t (m) is the pore close-off depth. ρ_s was set to 350 kg m^{-3}, obtained from observations at the snow pit, and z_t was set to 60 m, obtained from density measurements of the ice core. The stratigraphic features showed that the observation site should be categorized as a dry snow zone. The ice depth was converted to water-equivalent depth using the density profile. The water-equivalent depth at the bottom of the 222.72-m ice core was 186.1 m.

We then divided the ice-core segments longitudinally into two parts (part A: 60 %, part B: 40 %) with a band saw from the surface to 112.87-m depth. We removed ice chips on the cut surface of the part-A ice-core segments with a brush and took NIR photographs for a pilot study of ice layer detection and grain size measurement on the platform in a housing covered with a translucent cloth to supply homogeneous diffuse illumination conditions under solar radiation. For the NIR photographs, we used a Nikon D4 digital camera, which was adapted to detect NIR spectra with a 25-mm Zeiss ZF-IR lens and a gelatin filter (X-Nite 850 nm filter) that selected the wavelengths from 840 to 940 nm. Calibration targets consisted of three Spectralon grayscale standards with NIR reflectance values of 10 %, 55 %, and 99 % set around the measured part of the ice core. After taking the NIR image, the measured part was covered with a board of homogeneous simulated snow (white thermal insulating material), and we took an NIR image of the board under the same conditions as those used for the NIR image of the ice core. This image of the board was used for correction of spatial variation in illumination conditions in the original NIR image of the ice core. The details of the NIR photometry are provided in Yamaguchi *et al.* (2014b) and Matzl and Schneebeli (2006). After the photographs had been taken, the ice-core samples were packed into polyethylene bags and placed in insulated boxes for transport to Japan.

The part-B ice-core segments were cut latitudinally at 50- to 120-mm intervals, and each subsample was placed in a new polyethylene bag after the surface of the ice sample had been removed using a ceramic knife for decontamination. The subsamples were then melted in a water bath and decanted into pre-cleaned polypropylene bottles in a tent for sample melting, which was carried out at the windward side of the tent to prevent contamination from generator exhaust and the kitchen. The number of bottled samples was 2193. The bottled samples were kept frozen in snow during the field observations.

We processed the ice-core sections from 112.87 to 175.77 m using different procedures owing to a lack of time. The ice-core sections were cut in half longitudinally with a band saw. One side of the halved ice-core sections was placed in polyethylene bags and packed into insulated boxes for transport to Japan. From the other half, we collected 0.05-m-long ice subsamples at ~0.5-m depth intervals for heavy metal analysis, and placed each subsample in new polyethylene bags. The remaining part of each ice-core sample from the 0.5-m intervals was melted in a water bath and decanted into pre-cleaned polypropylene bottles.

The ice-core samples from 175.77 m to the core bottom were placed in polyethylene bags and packed into insulated boxes with no cutting processes for transport to Japan.

All ice-core samples were kept frozen until the samples were transported to the NIPR in Japan. All bottled samples were kept frozen until the samples were transported first to Qaanaaq, and then at ambient temperature from Qaanaaq to the Institute of Low Temperature Science, Hokkaido University (ILTS-HU), where they were kept frozen in a cold laboratory until the chemical analyses were performed.

6.4 Snow-pit observations

On 14 May, we conducted snow-pit observations down to a depth of 1.25 m. The observation variables were snow temperature, stratigraphy, and density (Fig. 5). Snow samples for chemical analysis were collected at 3-cm depth intervals using stainless-steel tools, and each sample was placed in a separate polyethylene bag. Samples for major ion and stable isotope analyses were melted in a water bath and decanted into pre-cleaned polypropylene bottles. Samples for heavy metals were collected at roughly 3- to 4-cm intervals using the same stainless-steel tools and then packed individually in new polyethylene bags.

On 21 May, we dug another snow pit to a depth of 2.5 m for NIR photometry analysis. After digging the snow pit, we smoothed the surface of the walls as much as possible with a single-edged snow saw and then covered the snow pit roof with translucent cloth (polyvinyl chloride, 1.5 mm thickness) to supply homogeneous diffuse illumination conditions under solar radiation. The observation system employed for NIR photometry was the same as that used for the ice core described in Section 6.3. For calibration of NIR reflectance, eight sets of the same three Spectralon grayscale standards used in the procedure with the ice core were placed on a rectangular metal frame in the observation zone of the snow-pit wall. The remainder of the procedure for the NIR photometry measurements was identical to that for the ice core.

6.5 Ice-velocity measurements

On 6 May, we installed an aluminum pole at the observation site and mounted the antenna of a dual-frequency GPS receiver (GNSS Technologies Inc., GEM-1). GPS satellite signals were recorded by the receiver every 1s from 6 to 26 May. The GPS data were post-processed with the static precise point positioning (PPP) method using an on-line software application (CSRS-PPP: http://webapp.geod.nrcan.gc.ca/geod/tools-outils/ppp.php) maintained by Natural Resources Canada. The horizontal velocity during the survey period was calculated as 2.59± 0.13 m a^{-1} (Fig. 6).

We also installed four additional poles at approximately 2 km north, south, east, and west from the observation site (Fig. 6). We used the same device to record GPS satellite signals for ～40 min on 11 and 26 May. The GPS data were post processed in static mode with data recorded at the drilling site as the reference station. The calculated velocities at the measurement sites are shown in Fig. 6.

6.6 Surface elevation

The ice sheet surface elevation was surveyed in the vicinity of the observation site by walking with a GPS receiver mounted on a sledge. We used the same GPS device and the reference station data to post-process the GPS data in kinematic mode. The surface elevation contours based on these measurements are shown in Fig. 6.

6.7 AWS installation

An automated weather station (AWS) was installed near the drilling site on 10 May (Fig. 7). The AWS measures the meteorological and snow parameters shown in Table 3. The new installation proceeded without complications, and everything is operating normally. The electrical power is supplied from cyclone batteries in the snow, which are charged by solar panels. For all instruments, 1-min sampling and 10-min averaged data are

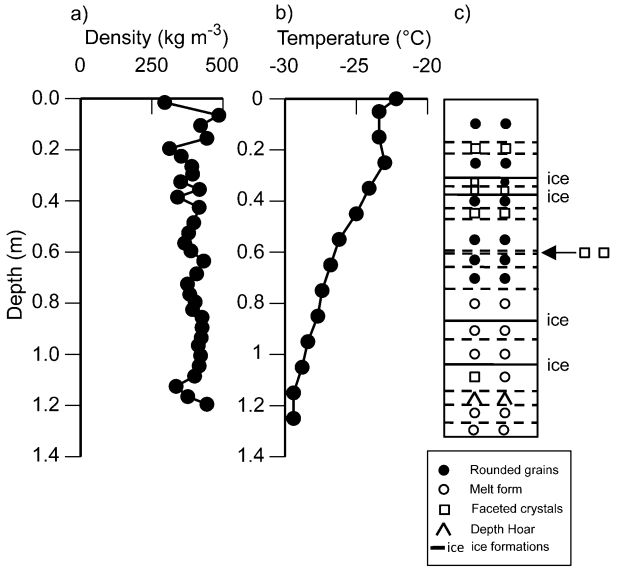

Fig. 5. Vertical profiles of snow density (a) and snow temperature (b), and snow stratigraphy in snow pit (c) on 14 May at SIGMA-D site. Broken lines in the figure (c) indicates boundaries of snow layers. An arrow in the figure (c) indicates the snow type in a thin layer at 0.68–0.69 m depth.

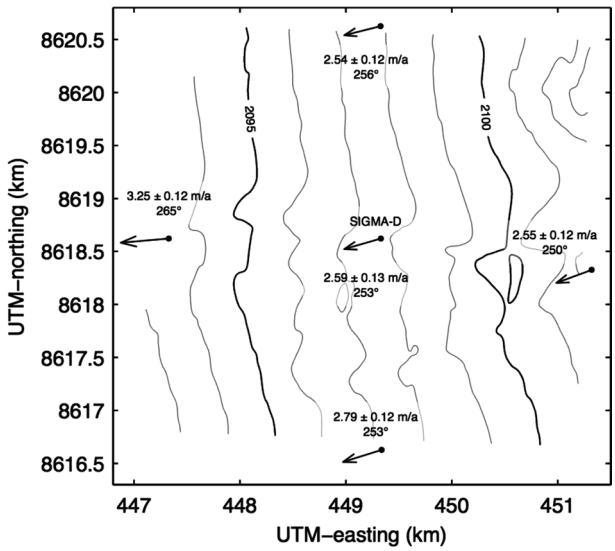

Fig. 6. Surface elevation measured by this study at contour intervals of 1 m, and locations of the flow velocity measurements (solid circles) and horizontal velocity vectors (arrows). Coordinates are in UTM zone 20N (km).

stored on a data logger, and 10-min averaged data are also transported to us via the Argos satellite. The data are available through the Antarctic Data System (ADS) website (http://ads.nipr.ac.jp/index.html) with free access.

6.8 Meteorological observations

We conducted meteorological observations three times daily during the field camp. Air temperature, air pressure, wind speed and direction was observed using a hand-held meteorological meter (Kestrel 4500NW), and cloud type, cloud amount, and visibility was observed by visual observation (Fig. 8). The minimum temperature during the observations was −33.3℃ at 06:30 on 7 May.

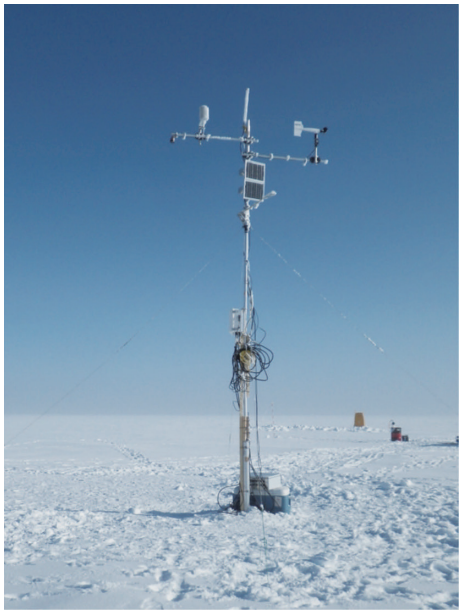

Fig. 7. AWS installed at SIGMA-D on 10 May 2014.

7. Concluding remarks

We drilled a 222.55-m ice core in an accumulation area of the northwestern GrIS where SIGMA and GRENE-Arctic are conducting glaciological and meteorological studies. We processed some of the ice-core samples and prepared liquid samples. The liquid samples were transported to the ILTS-HU and will be analyzed for water stable isotopes and soluble major ion concentrations at the ILTS-HU, tritium content at the National Institute of Polar Research (NIPR), and heavy metal concentrations at Yamagata University. The remaining ice-core samples were packed in insulated boxes, kept frozen, and transported to the NIPR. We plan to analyze black carbon, insoluble particles, water-stable isotopes, stable isotopes of strontium and neodymium, soluble-salt particles, and heavy metals. We also conducted borehole temperature measurements, a new pit study, a surface-elevation survey and ice-velocity measurements by GPS, and installed an AWS.

Acknowledgments

We thank Katsuyuki Kuchiki and Akihiro Hashimoto for their helpful support in Japan. We also thank Kenn Bohrek Air Ltd. and the Polar Continental Shelf Program in Resolute Bay for their support of our flight operations, and Sakiko Daorana, Finn Hansen, Jesper Olsen, Lars Wille, and Navaraga K'avigak for their logistical support in Qaanaaq. This study was supported in part by (1) a Japan Society for the Promotion of Science (JSPS) Grant-in-Aid for Scientific Research (S) number 23221004, (2) Grant-in-Aid for Scientific Research (C) number 26400460, (3) the Green Network of Excellence (GRENE) Arctic Climate Change Research Project, and (4) a grant from the Joint Research Program of the Institute of Low Temperature Science, Hokkaido University.

Table 3. AWS instruments at SIGMA-D.

Parameter	Height (m)[1]	Instrument
Air temperature and relative humidity	6.22	Thermo-hygrometer (HMP-155, Vaisala, Finland, and Multi-plate radiation shield Model-41003, Young Co., USA)
Air pressure	3.20 m	Barometer (PTB210, Vaisala, Finland)
Wind speed and direction	6.12	Aerovane (model-05130, Young Co., USA)
Snow height change	5.78	Ultrasonic snow gauge (SR50A, Campbell Scientific Inc., USA)
Downward and upward solar radiation	4.80	Net radiometer (CNR-4, Kipp & Zonen, Netherlands)
Downward and upward longwave radiation	4.80	Net radiometer (CNR-4, Kipp & Zonen, Netherlands)
Tilt angle of AWS main pole	4.69	Inclinometer (B2N85H, Turck Inc., USA)
Snow temperature	3.5, 2.9, 2.1, 1.1, 0, -0.5	Plutinum resistance thermometer (PTWP-10, Climatec Inc., Japan)
Data recording		Data logger (CR1000, Cambell Scientific Inc., USA)

[1] Values at the time of installation on 10 May 2014.

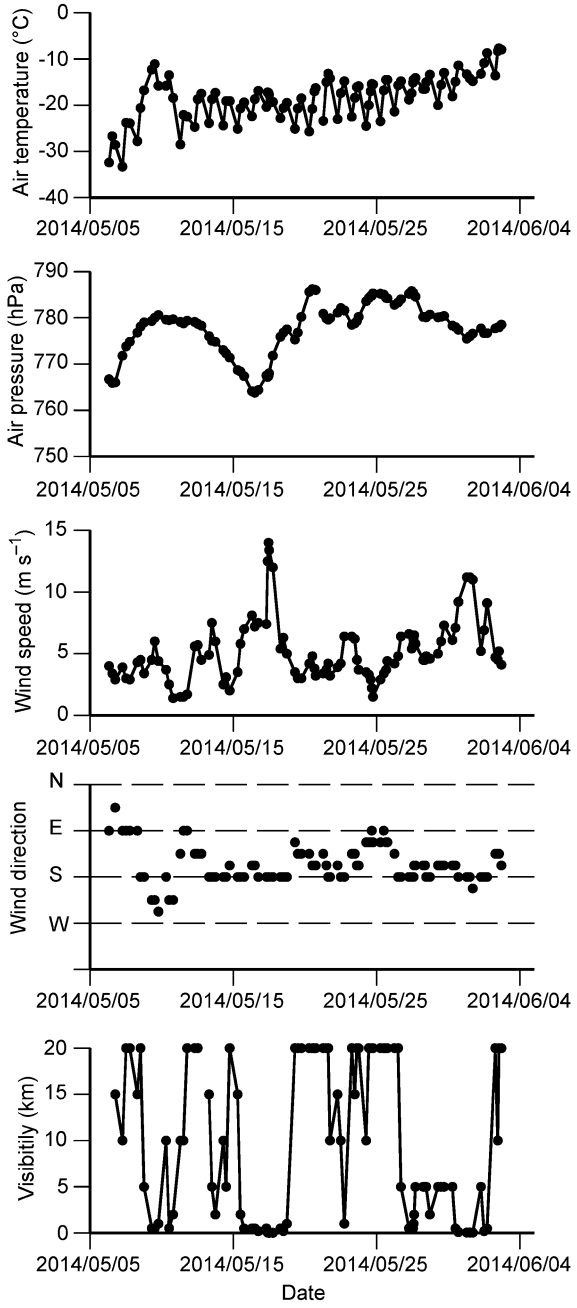

Fig. 8. Air temperature, air pressure, wind speed and direction, and visibility observed at SIGMA-D from 6 May to 2 June.

References

Aoki, T., Matoba, S., Uetake, J., Takeuchi, N. and Motoyama, H. (2014): Field activities of the "Snow Impurity and Glacial Microbe effects on abrupt waring in the Arctic" (SIGMA) Project in Greenland in 2011–2013. *Bull. Glaciol. Res.*, **32**, 3–20, doi: 10.5331/bgr.32.3.

Bales, R. C., McConnell, J. R., Mosley-Thompson, E. and Csatho, B. (2001): Accumulation over the Greenland ice sheet from historical and recent records, *J. Geophys. Res.*, **106**(D24), 33,813–33,825, doi:10.1029/2001 JD900153.

Enderlin, E. M., Howat I. M., Jeong S., Noh M-J, van Angelen J. H. and van den Broeke M. R. (2014): An improved mass budget for the Greenland ice sheet. *Geophys. Res. Lett.*, **41**(3), 866–872, doi: 10.1002/2013GL059010.

Kameda, T., Takahashi, S., Goto-Azuma, K., Kohshima, S., Watanabe, S. and Hagen, J. O. (1993): First report of ice core analyses and borehole temperatures on the highest icefield on western Spitsbergen in 1992. *Bull. Glaciol. Res.*, **11**, 51–61.

Khan, S. A., Kjær, K. H., Bevis, M., Bamber, J. L., Wahr, J., Kjeldsen, K. K., Bjørk, A. A., Korsgaard, N. J., Steams, L. A., van den Broeke, M. R., Liu L., Larsen N. K. and Muresan, I. S. (2014): Sustained mass loss of the northeast Greenland ice sheet triggered by regional warming. *Nature Climate Change*, **4**(4), 292–299, doi: 10.1038/ nclimate2161.

Koci, B. (2002): A review of high-altitude drilling. *Mem. Natl. Inst. Polar Res., Special Issue*, **56**, 1–4.

Matoba, S., Shimbori, K. and Shiraiwa, T. (2014): Alpine ice-core drilling in the North Pacific region. *Ann. Glaciol.*, **55**(68), 83–87, doi:10.3189/2014AoG68A020.

Matzl, M. and Schneebeli, M. (2006): Measuring specific surface area of snow by near-infrared photography. *J. Glaciol.*, **52**, 558–564. doi:10.3189/172756506781828412.

Motoyama, H., Watanabe, O., Goto-Azuma, K., Igarashi, M., Miyahara, M., Nagasaki, T., Karlof, L. and Isaksson, E. (2001): Activities of the Japanese Arctic Glaciological Expedition in 1999 (JAGE 1999). *Mem. Natl Inst. Polar Res., Spec. Issue*, **54**, 253–260.

Rignot, E. and Kanagaratnam, P. (2006): Changes in the velocity structure of the Greenland Ice Sheet. *Science*, **311**, 989–989, doi:10.1126/science.1121381

Rignot, E., Velicogna, I., van den Broeke, M. R., Monaghan, A. and Lenaerts, J. (2011): Acceleration of the contribution of The Greenland and Antarctic ice sheets to sea level rise. *Geophys. Res. Lett.*, **38**, L05503, doi:10.1029/2011GL046583.

Sasgen, I., van den Broeke, M., Bamber, J. L., Rignot, E., Sørensen, L. S., Woulter, B., Martinec, Z., Velicogna, I. and Simonsen, S. B. (2012): Timing and origin of recent regional ice-mass loss in Greenland. *Earth Planet. Sci. Lett.*, 333–334, 293–303, doi: 10.1016/j.epsl.2012.03.033.

Schytt, V. (1958): The inner structure of the ice shelf at Maudheim as shown by core drilling. *Norwegian-British-Swedish Antarctic Expedition, 1949–52*, Scientific Results 4, Glaciology 2. Norsk Polarinstitutt, Oslo, 115–151.

Shiraiwa, T., Goto-Azuma, K., Matoba, S., Yamasaki, T., Segawa, T., Kanamori, S., Matsuoka, K. and Fujii, Y. (2003): Ice core drilling at King Col, Mount Logan 2002. *Bull. Glaciol. Res.*, **20**, 57–63.

Sugiyama, S., Sakakibara, D., Matsuno, S., Yamaguchi, S., Matoba S. and Aoki, T. (2014): Initial field observations on Qaanaaq Ice Cap in northwestern Greenland. *Ann. Glaciol.* **55**(66), 25–33, doi: 10.3189/2014AoG66A102.

Sugiyama, S., Sakakibara, D., Tsutaki, S., Maruyama, M. and Sawagaki, T. (2015): Glacier dynamics near the calving front of Bowdoin Glacier, northwestern Greenland. *J. Glaciol.*, **61**, 223–232, doi: 10.3189/2015 JoG14 J127.

Takahashi, A. (1996): Development of a new shallow ice core drill. *Seppyo*, **58**(1), 29–37 [in Japanese with English summary].

van den Broeke, M., Bamber, J., Ettema, J., Rignot, E., Schrama, E., van de Berg, W. J., van Meijgaard, E., Velicogna, I. and Wouters., B. (2009): Partitioning recent Greenland mass loss, *Science*, **326**, 984–986, doi: 10.1126/science.1178176.

Yamaguchi, S., Matoba, S., Yamasaki, T., Tsushima, A., Niwano, M., Tanikawa, T. and Aoki, T. (2014a): Glaciological observations in 2012 and 2013 at SIGMA-A site, Northwest Greenland. *Bull. Glaciol. Res.*, **32**, 95–105, doi: 10.5331/bgr.32.95.

Yamaguchi, S., Motoyoshi, H., Tanikawa, T., Aoki, T., Niwano, M., Takeuchi, Y., Endo, Y. (2014b): Application of snow specific surface area measurement using an optical method based on near-infrared reflectance around 900-nm wavelength to set snow zones in Japan. *Bull. Glaciol. Res.*, **32**, 55–64, doi: 10.5331/bgr.32.55.